

Selection of a DNA aptamer for aflatoxin B1 (AFB1) and the development of a lateral flow assay (LFA) for the detection of aflatoxins in spiked peanut extract

Fiona Ebanks, Erin M. McConnell, Emily Mastronardi, Daniel Goudreau, Hadi Nasrallah, Maria C. DeRosa,^a

^a Laboratory for Aptamer Discovery and Development of Emerging Research (LADDER), Department of Chemistry, Carleton University, 1125 Colonel By Dr., Ottawa, ON, K1S 5B6, Canada

Supplemental

Materials and methods

Chemicals and instruments

Unmodified DNA sequences were synthesized using standard phosphoramidite chemistry using a BioAutomation MerMade 6 oligonucleotide synthesizer (Plano, TX, USA). Phosphoramidites (dA-CE, Ac-dC-CE, dmf-dG-CE, and dT-CE), activator, deblock, cap A/B, oxidizer, 2.0 M triethylamine acetate (TEAA) and anhydrous acetonitrile were purchased from Glen-Research (Sterling, VA, USA). Synthesis grade acetonitrile was purchased from BDH VWR Analytical (Mississauga, ON, CA). 1000 Å size-controlled glass pore (CGP) columns were purchased from LGC Biosearch Technologies (Alexandria, MN, USA). Biotin and cyanine-5 modified HPLC purified DNA aptamers were purchased from IDT DNA Technologies (Coralville, Iowa, USA). Bis-acrylamide 40% solution, electrophoresis grade ammonium persulfate, N,N,N',N'-tetramethylethylenediamine (TEMED), ethylenediaminetetraacetic acid (EDTA), Boric acid, tris(hydroxymethyl) aminomethane (Tris) and urea were all purchased from Bioshop Canada Inc. Amicon-Ultra 0.5 mL 3 kDa centrifugal filters were purchased from Sigma-Aldrich. PAGE gels were imaged using an Alpha Innotech multi-image light cabinet. Gold (III) chloride trihydrate (HAuCl₄·3H₂O, ≤99.9%), aflatoxin B1, B1, G1, G2, ochratoxin A, fumonisins B1, atrazine, and deoxynivalenol were purchased from Sigma Aldrich (St. Louis, MO, USA). Buffer components were purchased from BioShop (Burlington, ON, CA). Nitric acid, hydrochloric acid and ammonium hydroxide were purchased from Anachemia (VWR, Mississauga, ON, CA). Mesh copper TEM grids (300 x 83 μm) were purchased from Electron Microscopy Sciences (Hatfield, Pennsylvania, USA). The absorption pad (CFSP223000) was obtained from Millipore (Bedford, MA, USA). Pullulan was bought from Polysci (Warrington, PA, USA). The nitrocellulose (NC) membrane was purchased from Sartorius Stedim Biotech (Goettingen, Germany). For MST analysis, NanoTemper (Munich, Germany) MO-K022 capillaries were used.

Instrumentation

Ultraviolet-visible spectra were recorded using the Varian Cary Bio 300 UV-Vis spectrometer (Varian, Santa Clara, CA, USA). High-resolution transmission electron microscopy (HR-TEM) was done using an FEI Technai G2 F20 TEM at the Carleton University Nano-imaging Facility, with a field emission source at a voltage of 200 kV using Gatan Microscopy Suite 2V (Carleton University, Ottawa, ON, CA). The GeBIODOT's BIODOT: dispensing platform ZX 1000 was used to print LFAs. Digital photographs were taken using an iPhone. Quantitative analysis of the LFA strips was done using ImageJ software, and statistical analysis was done using GraphPad Prism 10. Sequence structure and binding were monitored by circular dichroism (CD) using the JASCO (J-815) CD Spectrometer (Easton, MD, USA) and by microscale thermophoresis (MST) using the Monolith NT.115 Pico (Munich, Germany)

Colorimetric assay development

Synthesis of Gold Nanoparticles and characterization

AuNP preparation was adapted from Graber et al.,¹ with changes to the volume of HAuCl_4 and sodium citrate to yield larger colloids. Prior to use, all glassware was soaked in aqua regia (3:1 mixture of concentrated HCl/HNO_3) for 15 minutes, then rinsed thoroughly with deionized water. In a 250 mL Erlenmeyer flask, 98 mL of deionized water and 2 mL of 50 mM HAuCl_4 were mixed to a final concentration of 1 mM HAuCl_4 . The solution was covered to prevent evaporation and heated to boiling with stirring. Upon boiling, 10 mL of 38.8 mM sodium citrate was added, resulting in a colour change from pale yellow to purple and then to wine red. The nanoparticle solution was removed and cooled at room temperature prior to storage at 4°C. The nanoparticles were quantified by UV-Vis spectrometry. Size and composition analysis was done by drying 10 μL of the AuNP solution onto a copper-coated carbon nano-grid prior to HR-TEM analysis.

Capture-SELEX process

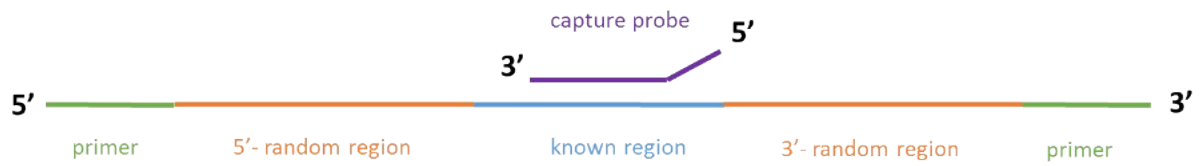


Figure S1: General template design of the selection library highlighting the primer regions (green), the two random regions (orange) and a central known region (blue). The complementary capture probe is highlighted in purple.

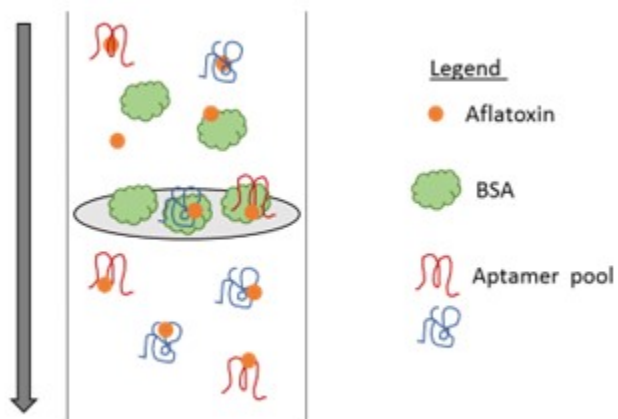


Figure S2: Filtration of aflatoxin binding aptamers from the complex matrix. Abbreviations: Bovine serum albumin (BSA).

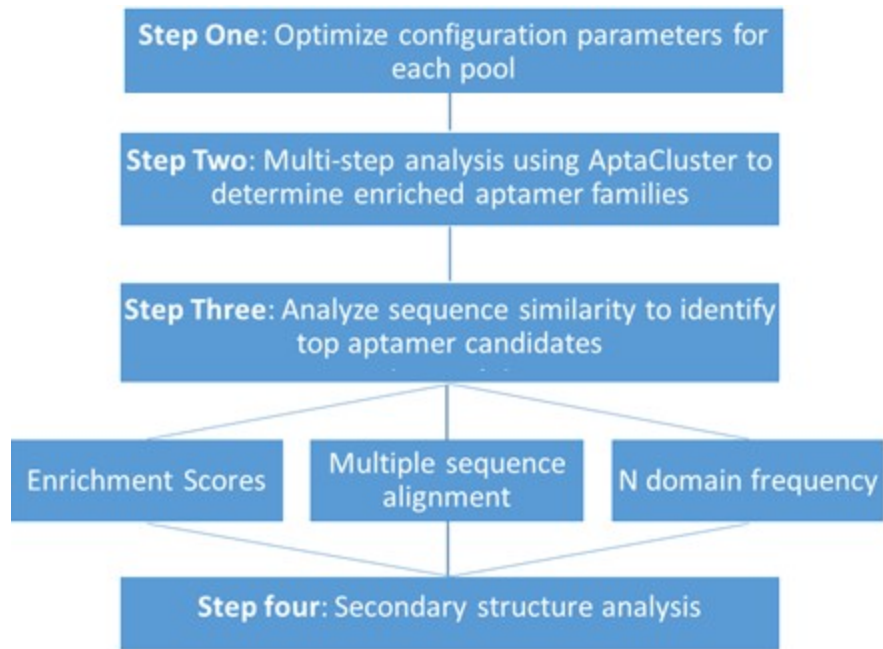


Figure S3: Work-flow analysis of high-throughput sequencing data

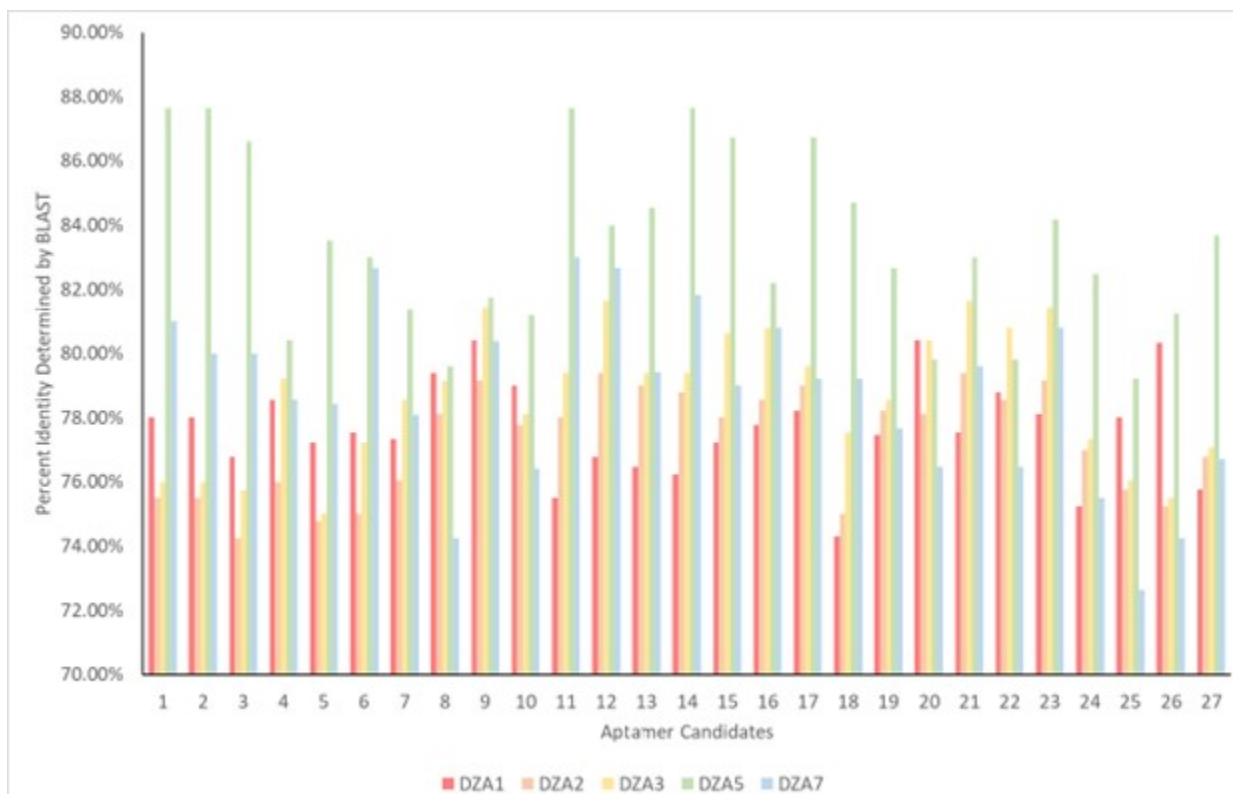


Figure S4: Percent Identity Comparison of DZA aptamer candidates to the remainder of the top 32 Sequences, chosen based on enrichment, count, family representation, and predicted secondary structure.

Preliminary specificity screening of promising aptamer candidates

As a preliminary assessment of selectivity, the top aptamer candidates (DZA_3, DZA_5 and DZA_7) were examined for their affinity to the counter-toxins OTA, DON, FB1 and zearalenone. Due to strict regulations T2 toxin was not available for selections or characterization assays. The concentration of each counter target toxin was 0.05 μ M (DON:14.82 ppb, FB1: 36.09 ppb, OTA: 20.19 ppb and Z: 15.92 ppb). The affinity of each aptamer candidate for each toxin was screened separately. Fluorescent images of the aptamer candidate screening are shown in Fig. S4. Since there were no obvious differences in the fluorescence intensity between the control bands (C) and any of the counter target toxin reactions visually, the SpotDenso feature was used to analyze the fluorescent gel images. Differences in the background corrected intensities of the top and bottom bands were compared for candidates but there was insufficient evidence to suggest that any of the candidates bind to the counter targets. Just as the affinity of an aptamer for its target can change depending on the conditions it is examined in, so too can the affinity of the aptamer for counter targets. For instance, the affinity of the aptamer for a counter target may not be strong enough to disrupt the aptamer-capture probe interaction, but binding may be observed in the absence of the capture probe. Though preliminary screening of aptamer selectivity is promising, it is necessary to evaluate the cross-reactivity of the chosen aptamer candidates in the final application.

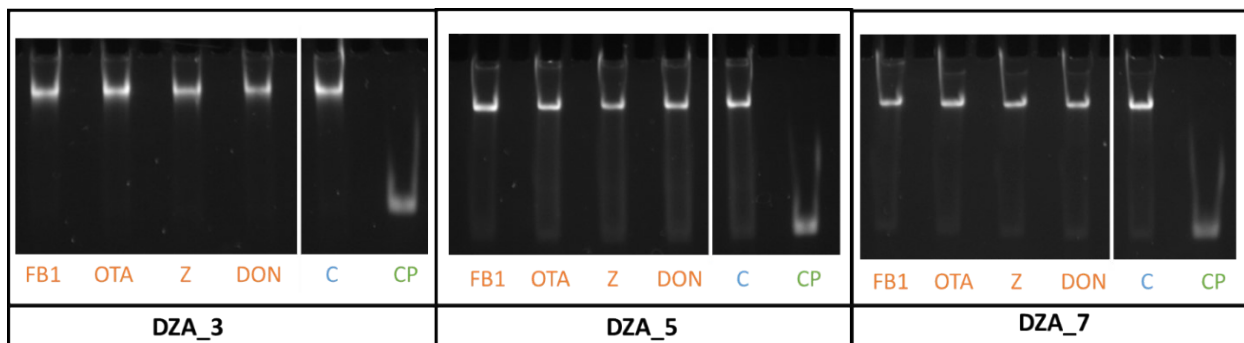


Figure S5: Counter-target affinity screening of DNzyme aptamer candidates (DZA). Abbreviations: fumonisins (FB1), ochratoxin a (OTA), zearalenone (Z), deoxynivalenol (DON), hybridization reaction control (C), capture probe (CP). Control reactions are separated by a white line.

Microscale thermophoresis

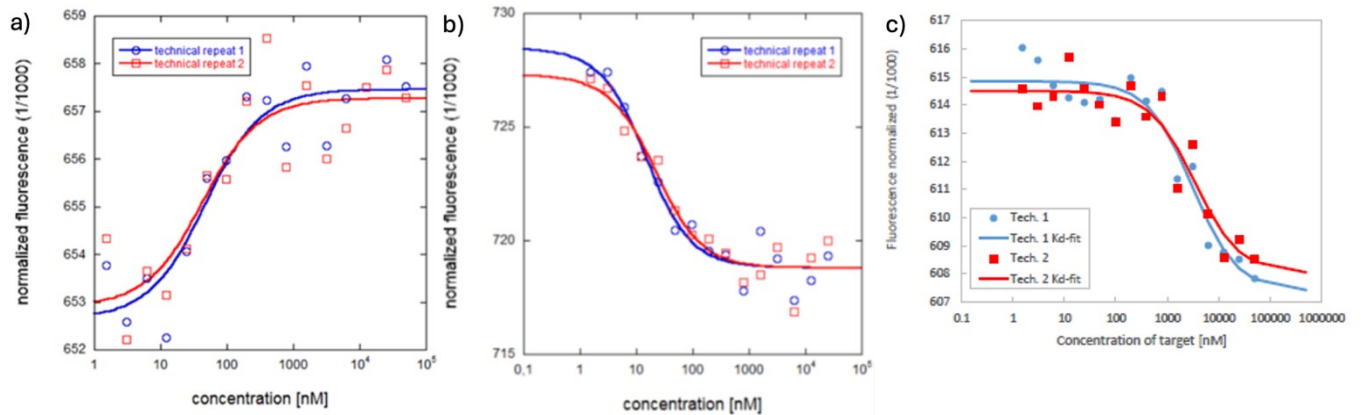


Figure S6: MST traces normalized fluorescence for a) DZA3 challenged with AFB1 resulting in a K_d of 41.1 ± 23.8 nM, b) DZA3 challenged with AFG2 resulting in a K_d of 15.3 ± 4.8 , and DZA7 challenged with AFB2 resulting in a K_d of 3.3 ± 0.2 μ M.

Structural prediction

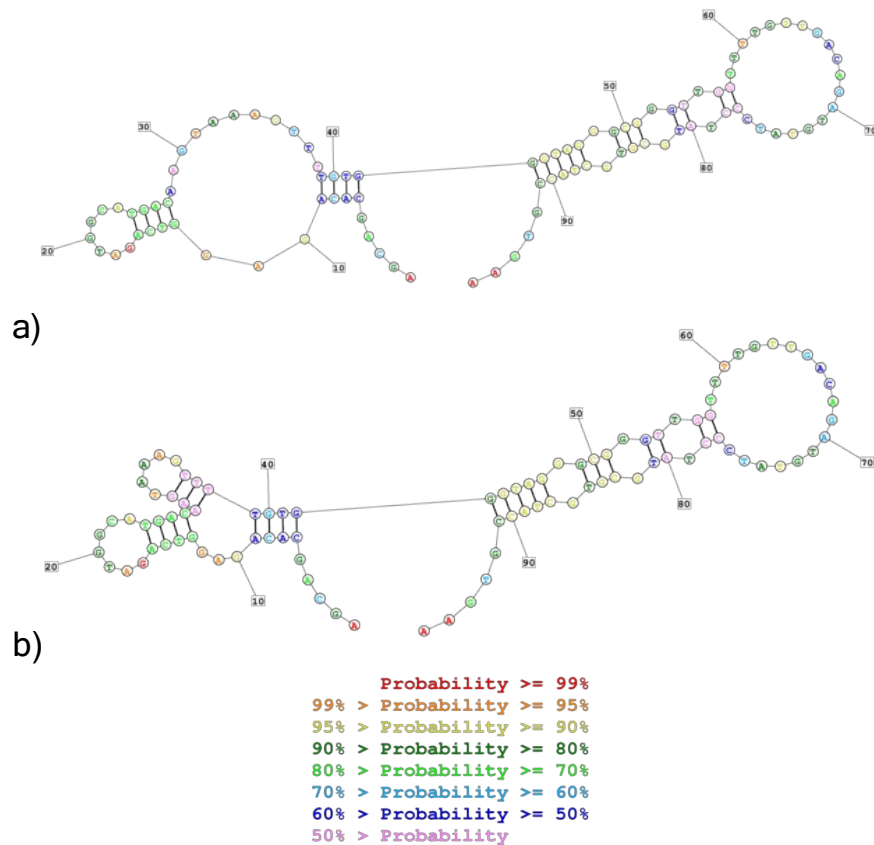
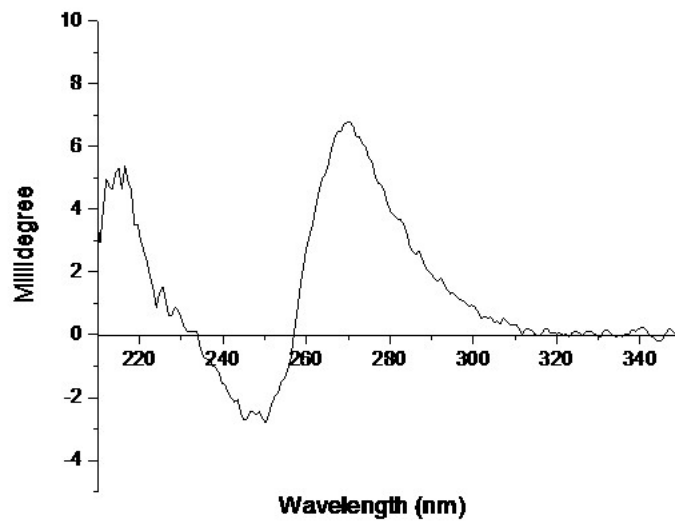


Figure S7: The secondary structures of DZA3 were predicted by RNAstructure.⁶¹ a) Shows the secondary structure predicted by MaxExpect, and b) shows the secondary structure predicted by the minimum folding free energy. The colour-coded index represents the probability of the base pair in percent.



Circular dichroism

Figure S8: CD spectrum of parallel-stranded G-quadruplex forming PS2.M sequence in 20 mM Tris buffer (100 mM NaCl, 5 mM KCl, 1mM CaCl₂, 1 mM MgCl₂), as monitored by UV-CD using an Olis Cary 17 CD spectropolarimeter.

Preparation of colorimetric assays

The appropriate concentration of AuNP was determined by visual clarity and UV-Vis spectroscopy signal. This was done by evaluating AuNPs concentrations of 2.3, 2.9, 3.2, 3.5 and 4.1 nM by eye and by UV-Vis. To achieve this, aliquots of an 11.6 nM stock of AuNPs were mixed with an appropriate volume of water to achieve a final volume of 200 μ L. Eighty (80) μ L of the solution was placed in a 10mm quartz cuvette and ran on a Cary Bio 300 UV-Vis Spectrometer, monitoring the absorbance at 520 nm.

A series of salt and aptamer optimizations were then conducted to determine the concentrations of sodium chloride (NaCl), and aptamer required for the colorimetric assay experiment. NaCl optimization was done by adding aliquots of 0.3 M NaCl solution to 3.5 nM AuNP, and the changes in absorbance at 520 nm and 640 nm were monitored. Aptamer optimization was conducted by assessing the ability of various aptamer concentrations to protect the AuNP surface from aggregation by NaCl. One (1) to 10 μ L of a 10 μ M stock of aptamer was tested with 3.5 nM AuNP and 0.08 M NaCl and monitored by eye. An aptamer concentration of 0.4 nM was deemed sufficient to passivate the surface of AuNP. Further optimization of the AuNP and NaCl concentrations was done, and a final concentration of 2.95 nM AuNP and 0.06 M NaCl were chosen. This was followed by an analysis of the AuNPs alone in the presence of AFB1 to determine the probability of false positives. To do this, 0.33 μ M to 10 μ M AFB1 was added to 2.95 nM AuNP and changes in colour were monitored.

In-solution colorimetric assay and control

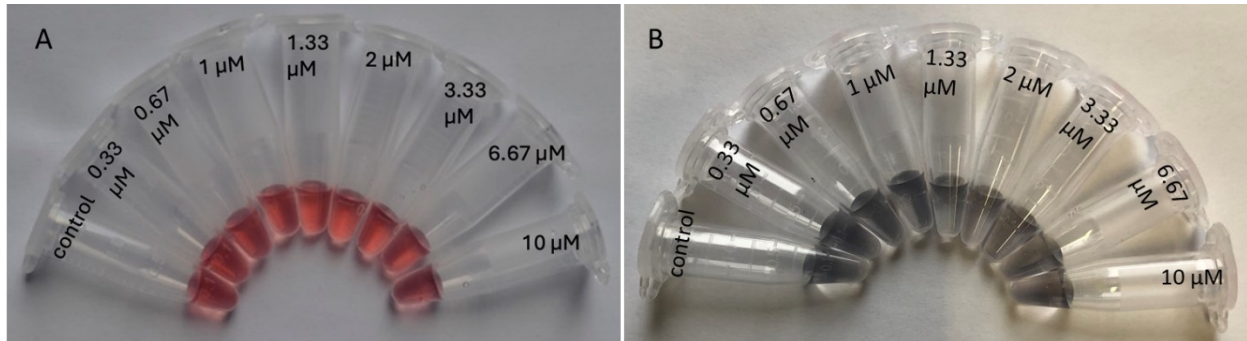


Figure S9: A) Various concentrations of AFB1 with AuNPs to determine if AFB1 can aggregate the AuNPs independently. At concentrations above 10 μM AFB1, the AuNPs AFB1 induces the aggregation of the AuNPs. B) Various concentrations of AFB1 with AuNPs and NaCl to determine if the AFB1 has a protective effect against nanoparticle aggregation.

Calculation of limit of detection (LOD) and limit of quantification (LOQ)

$$LOD = \frac{3.3 \times Sy.x}{slope}$$

$$LOQ = \frac{10 \times Sy.x}{slope}$$

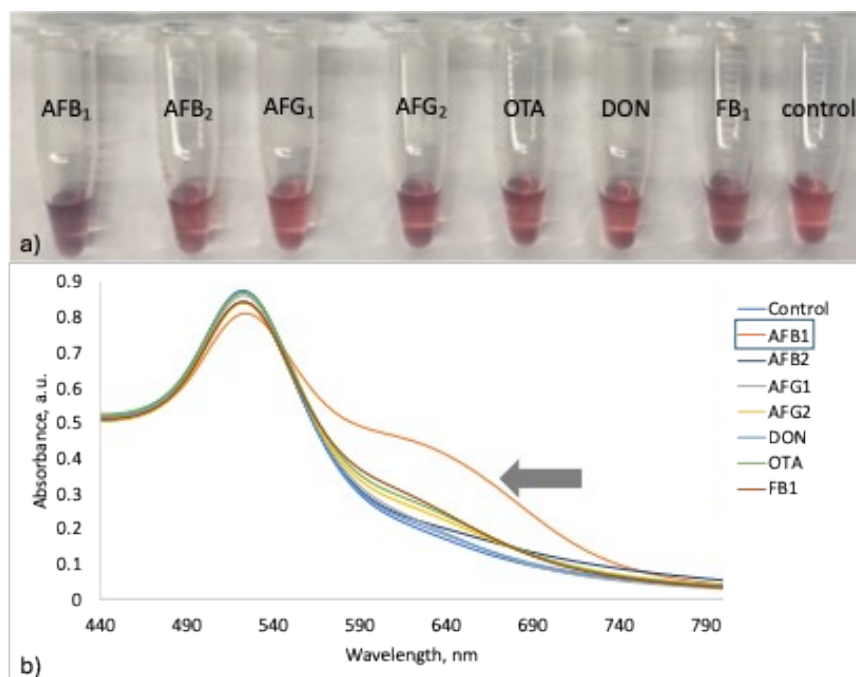


Figure S10: a) Image 10 μ M AFB₁, AFB₂, AFG₁, AFG₂, OTA, DON, FB₁, and control (no target) showing the significant colour change in the presence of AFB₁ and b) Spectral changes to AuNP due to the aptamer's interaction with varying 10 μ M AFB₁, AFB₂, AFG₁, AFG₂, OTA, DON, FB₁. Control (no target).

The solution-based colorimetric assay was performed in the presence of 10 μ M of each mycotoxin. As observed in Fig. S8, AFB₁, AFG₂, OTA and FB₁ showed signs of AuNPs aggregation, with AFB₁ being the most prominent. Little AuNP aggregation was observed in the other control toxins. The samples were further analysed by UV-Vis spectroscopy. In the presence of AFB₁, there was a prominent absorbance peak at 640 nm and a reduced peak intensity at 520 nm, confirming the affinity of the aptamer to AFB₁. There were also smaller absorbance peaks at 640 nm in the presence of AFG₂, OTA and FB₁. Some interaction with any of the congeners of AFs is to be expected because DZA3 was selected as a total aflatoxins aptamer. Aptamers fold into unique three-dimensional structures that are complementary to the shape and charge distribution of their target molecules. This allows them to form specific hydrogen bonds, electrostatic interactions, and hydrophobic contacts with the target.² Due to the functional groups on OTA and FB₁ and the increased concentration of toxin used, it is possible that there was non-specific binding to these molecules.

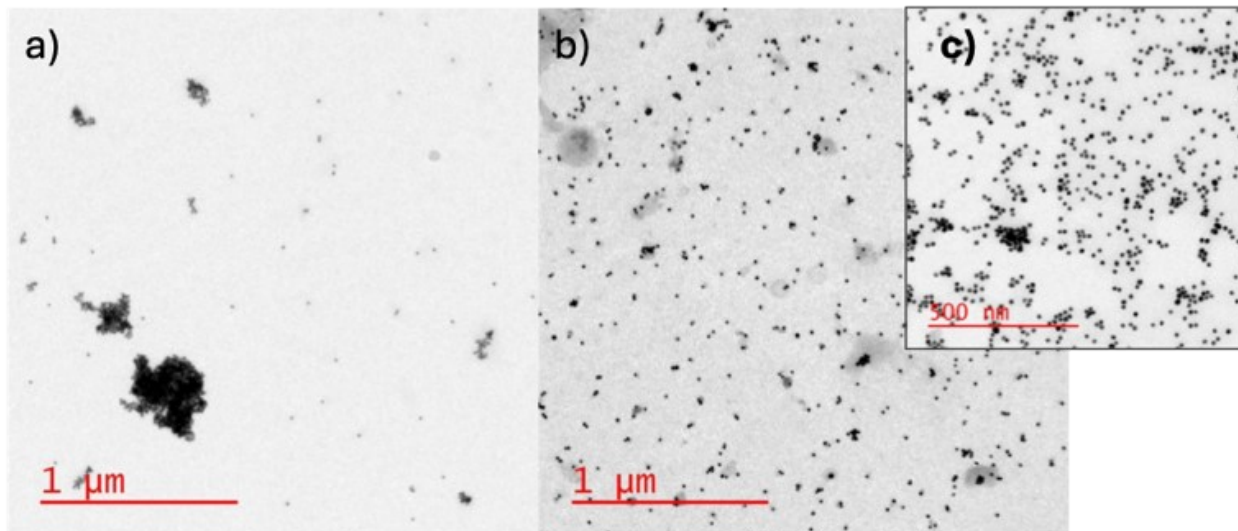


Figure S11: High-resolution TEM images showing a) the aggregation of AuNPs because DZA3 bound 10 μ M AFB1 in the presence of NaCl, b) the well-dispersed AuNPs in the absence of AFB1, highlight the stable aptamer-AuNP nanocomplex, and c) the magnified view of image (b).

Table S1: Summary of selection conditions by round.

Selection Round	DNA (pmol)	Counter (pmol)*	Total Aflatoxin ** (pmol)	Aflatoxin (ppb)	Notes on stringency
1	2000	N/A	57.8	B1: 2.03; B2: 5.97; G1: 20.35; G2: 18.83	DNA to aflatoxin ratio high to ensure candidates identified
2	450	8	3.2	B1: 1.56; B2: 0.31; G1: 0.33; G2: 0.33	Counter selection introduced and DNA:aflatoxin ratio decreased
3	400	8	3.2	B1: 1.56; B2: 0.31; G1: 0.33; G2: 0.33	DNA decreased
4	400	8	1.6	B1: 0.78; B2: 0.16; G1: 0.16; G2: 0.17	Aflatoxin decreased
5	400	8	1.6	B1: 0.78; B2: 0.16; G1: 0.16; G2: 0.17	Selection in complex matrix (5% BSA and corn extract)

*Deoxynivalenol (DON), fumonisin B1 (FB1), ochratoxin A (OTA) and zearalenone (5 nM each; 1.48, 3.61, 2.02 and 1.59 ppb respectively)

** 57.8 pmol corresponds to B1: 6.5 nM, B2: 19 nM, G1: 62 nM and G2: 57 nM. 3.2 pmol corresponds to 5 nM B1 and 1 nM B2, G1 and G2. 1.6 pmol corresponds to 2.5 nM B1 and 0.5 nM B2, G1 and G2, in solution respectively.

Table S2: Top Full length aptamer candidate sequences of interest from the DZA template. Common motifs are colour coded. Common regions (primers and capture region) are shown in black text, the exception being where the dark purple motif and the light orange motif appear in the capture region and 3'-primer respectively. Sequences are grouped into families based on motif similarity.

Sequence Candidates (5'→3')	
Template	5'-AGCAGCACAGAGGTCAGATG-N15-TTTTGTGGGTAGGGCGGGTTGGTTTT-N15-CCTATGCGTGCTACCGTGAA-3'
Scrambled Control	5-GAAGAAGAGCGACTCGTTACAAGATCAGGAGACGATTTTGTGGGTAGGGCGGGTTGGTTTTGACCTTCTCCGACGATGGTATGCAATAGATCGTGT-3'
Top Sequences of Interest	
DZA1.	AGCAGCACAGAGGTCAGATGAAATTTAATCTGACCTTTTGTGGGTAGGGCGGGTTGGTTTTATAGAAACCAACAGCCCTATGCGTGCTACCGTGAA
DZA2.	AGCAGCACAGAGGTCAGATGGCATGACAAGTAAAGTTTGTGGGTAGGGCGGGTTGGTTTTATAGAAACCAACAGCCCTATGCGTGCTACCGTGAA
DZA3.	AGCAGCACAGAGGTCAGATGGCATGACAAGTAAAGTTTGTGGGTAGGGCGGGTTGGTTTTGTTGACAGATGTATCCCTATGCGTGCTACCGTGAA
DZA5.	AGCAGCACAGAGGTCAGATGATACATCTGTCAACTTTTGTGGGTAGGGCGGGTTGGTTTTGACATCTGACCTCTGCCTATGCGTGCTACCGTGAA
DZA7.	AGCAGCACAGAGGTCAGATGATACATCTGTCAACTTTTGTGGGTAGGGCGGGTTGGTAGAGTGTAGATCTCGGTGCCTATGCGTGCTACCGTGAA
Remaining Top Sequences Grouped into Families	
1.	AGCAGCACAGAGGTCAGATGATCTAGTCCCCTCCTTTTGTGGGTAGGGCGGGTTGGTGATGGCATCTGACCTCTGCCTATGCGTGCTACCGTGAA
2.	AGCAGCACAGAGGTCAGATGATCTAGTCCCCTCCTTTTGTGGGTAGGGCGGGTTGGTCTTACCATCTGACCTCTGCCTATGCGTGCTACCGTGAA
3.	AGCAGCACAGAGGTCAGATGATCTAGTCCCCTCCTTTTGTGGGTAGGGCGGGTTGGTCGCTACATCTGACCTCTGCCTATGCGTGCTACCGTGAA
6.	AGCAGCACAGAGGTCAGATGATCTAGTCCCCTCCTTTTGTGGGTAGGGCGGGTTGGTACCATCTGACCTCTGTGCCCTATGCGTGCTACCGTGAA
5.	AGCAGCACAGAGGTCAGATGATCTAGTCCCCTCCTTTTGTGGGTAGGGCGGGTTGGTTCTGACCTCTGTGCTGCTCCTATGCGTGCTACCGTGAA
4.	AGCAGCACAGAGGTCAGATGATCTAGTCCCCTCCTTTTGTGGGTAGGGCGGGTTGGTTTTAAAATAGTTGTTATACCTATGCGTGCTACCGTGAA
7.	AGCAGCACAGAGGTCAGATGTAAACTCAACAGGAGTTTGTGGGTAGGGCGGGTTGGTATCTGACCTCTGTGCTGCTCCTATGCGTGCTACCGTGAA
8.	AGCAGCACAGAGGTCAGATGTAAACTCAACAGGAGTTTGTGGGTAGGGCGGGTTGGTTCCGATCTTACCTGCCACCCTATGCGTGCTACCGTGAA
9.	AGCAGCACAGAGGTCAGATGTAAACTCAACAGGAGTTTGTGGGTAGGGCGGGTTGGTTGCATCTGACCTCTGTGCCCTATGCGTGCTACCGTGAA
20.	AGCAGCACAGAGGTCAGATGTAAACTCAACAGGAGCAGTGTGGGTAGGGCGGGTTGGTTTTATCTGACCTCTGTGCCCTATGCGTGCTACCGTGAA
10.	AGCAGCACAGAGGTCAGATGTAAACTCAACAGGAGTTTGTGGGTAGGGCGGGTTGGTTCTGACCTCTGTGCTGCTCCTATGCGTGCTACCGTGAA
25.	AGCAGCACAGAGGTCAGATGTAAACTCAACAGGAGCAGTGTGGGTAGGGCGGGTTGGTTTTGACCTCTGTGCTGCTCCTATGCGTGCTACCGTGAA
11.	AGCAGCACAGAGGTCAGATGGGTAATAAGAACGAATTTTGTGGGTAGGGCGGGTTGGTAGCGCCATCTGACCTCTGCCTATGCGTGCTACCGTGAA
14.	AGCAGCACAGAGGTCAGATGGGTAATAAGAACGAATTTTGTGGGTAGGGCGGGTTGGTTCGACCATCTGACCTCTGCCTATGCGTGCTACCGTGAA
12.	AGCAGCACAGAGGTCAGATGGGTAATAAGAACGAATTTTGTGGGTAGGGCGGGTTGGTCCATCTGACCTCTGTGCCCTATGCGTGCTACCGTGAA
21.	AGCAGCACAGAGGTCAGATGGGTAATAAGAACGAACCATGTGGGTAGGGCGGGTTGGTTTTATCTGACCTCTGTGCCCTATGCGTGCTACCGTGAA
13.	AGCAGCACAGAGGTCAGATGGGTAATAAGAACGAATTTTGTGGGTAGGGCGGGTTGGTTCTGACCTCTGTGCTGCTCCTATGCGTGCTACCGTGAA
24.	AGCAGCACAGAGGTCAGATGGGTAATAAGAACGAACCATGTGGGTAGGGCGGGTTGGTTTTGACCTCTGTGCTGCTCCTATGCGTGCTACCGTGAA
15.	AGCAGCACAGAGGTCAGATGGGGAAAGGTCATGCGTTTTTGTGGGTAGGGCGGGTTGGTTCGGTCACTGACCTCTGCCTATGCGTGCTACCGTGAA
16.	AGCAGCACAGAGGTCAGATGGGGAAAGGTCATGCGTTTTTGTGGGTAGGGCGGGTTGGTCCATCTGACCTCTGTGCCCTATGCGTGCTACCGTGAA
17.	AGCAGCACAGAGGTCAGATGGGGAAAGGTCATGCGTTTTTGTGGGTAGGGCGGGTTGGTCTTACCATCTGACCTCTGCCTATGCGTGCTACCGTGAA
18.	AGCAGCACAGAGGTCAGATGGGGAAAGGTCATGCGTTTTTGTGGGTAGGGCGGGTTGGTGCACCCATCTGACCTCTGCCTATGCGTGCTACCGTGAA
19.	AGCAGCACAGAGGTCAGATGGGGAAAGGTCATGCGTTTTTGTGGGTAGGGCGGGTTGGTTCTGACCTCTGTGCTGCTCCTATGCGTGCTACCGTGAA
22.	AGCAGCACAGAGGTCAGATGGGGAAAGGTCATGCGGTCATGCGTTTTTGTGGGTAGGGCGGGTTGGTTTTATCTGACCTCTGTGCCCTATGCGTGCTACCGTGAA
23.	AGCAGCACAGAGGTCAGATGGTAATCCACGCTCTTTTATGTGGGTAGGGCGGGTTGGTTTTATCTGACCTCTGTGCCCTATGCGTGCTACCGTGAA
27.	AGCAGCACAGAGGTCAGATGGTAATCCACGCTCTTTTATGTGGGTAGGGCGGGTTGGTTTTGACCTCTGTGCTGCTCCTATGCGTGCTACCGTGAA
26.	AGCAGCACAGAGGTCAGATGGCACCCGCATCGTCCATGTGGGTAGGGCGGGTTGGTTTTGACCTCTGTGCTGCTCCTATGCGTGCTACCGTGAA

Table S3: Percent Identity Matrix Comparison of Top 5 Aptamer Candidates of Interest. Based on the 96-base template, there are 66 fixed bases; therefore, anything with a percent identity greater than 68.75% (66/96) shows enriched similarity.

	DZA1	DZA2	DZA3	DZA5	DZA7
DZA1	100.00	90.62	81.25	79.80	76.04
DZA2	90.62	100.00	90.62	82.18	78.57
DZA3	81.25	90.62	100.00	83.67	80.61
DZA5	79.80	82.18	83.67	100.00	88.78
DZA7	76.04	78.57	80.61	88.78	100.00

Table S4: Identity and concentrations of compounds and composition of total aflatoxins mixture used for control experiments.

Toxin	Composition	Concentration	
		nM	ppb
AFB1		50	15.61
AFs	AFB1	35	10.93
	AFB2	5	1.56
	AFG1	5	1.57
	AFG2	5	1.64
Deoxynivalenol (DON)		50	14.82
Ochratoxin A (OTA)		50	20.19
Fumonisin B1 (FB1)		50	36.09
Atrazine (ATR)		50	10.78

Table S5: Aptamers for AFB1 and AFM1

Aptamer and Target	Kd (buffer or complex)	Assessed in spiked/real samples?	Biosensor	Kd Method and Reference
AFB1				
DZA3	42.1 ± 23.8 nM (buffer)	Spiked peanuts	Colorimetric (AuNP on LFA)	MST; This work
DNA1	qPCR: 58.9 nM (buffer) and impedimetric: 43.7 nM (buffer)	Spiked peanuts	Electrochemical impedimetric	qPCR and impedimetric ³
fl-2CS1	2.5 μM (buffer)	Spiked peanuts	qPCR	ITC ⁴
AFB-8	18.54 ± 7.54 nM (buffer)	Spiked rice	Colorimetric (AuNP in solution)	Fluorescence ⁵
AFAB3	96.6 ± 8.6 nM (buffer)	not assessed	Not evaluated	Fluorescence ⁶
Aptamer 1	11.39 ± 1.27 nM (buffer)	Spiked peanut oil	Fluorescent Bioassay	Fluorescence ⁷
Patented aptamer by Neoventures Biotechnology	Typically nM (buffer)	Not disclosed	Not disclosed	Multiple methods ⁸
BSA conjugated AFB1				
AFLA5	50.45 ± 11.06 nM (buffer)	Spiked corn	ELONA and HPLC	ELONA ⁹
AFM1				
Aptamer 9	09.10 ± 6.02 nM (buffer)	Spiked powdered milk	Colorimetric (TMB in solution)	Fluorescence Polarisation ¹⁰
Apt-5	8.12 ± 1.51 nM (buffer)	Spiked milk	Colorimetric (AuNP in solution)	BLI ¹¹
AFAS3	35 nM (buffer)	Not assessed	Colorimetric (AuNP in solution)	Fluorescence ⁶

Abbreviations: 3,3',5,5'-tetramethylbenzidine (TMB), aflatoxin B1 (AFB1), aflatoxin M1 (AFM1), biofilm interferometry (BLI), bovine serum albumin (BSA), enzyme linked oligonucleotide assay (ELONA), fluorescence polarization (FP), gold nanoparticles (AuNPs), high performance liquid

chromatography (HPLC), isothermal calorimetry (ITC), lateral flow assay (LFA), microscale thermophoresis (MST), quantitative PCR (qPCR).

References

1. Grabar KC, Freeman RGriffith, Hommer MB, Natan MJ. Preparation and Characterization of Au Colloid Monolayers. *Anal Chem*. 1995;67(4):735-743. doi:10.1021/ac00100a008
2. Brown A, Brill J, Amini R, Nurmi C, Li Y. Development of Better Aptamers: Structured Library Approaches, Selection Methods, and Chemical Modifications. *Angewandte Chemie*. 2024;136(16). doi:10.1002/ANGE.202318665
3. Chang KY, Hong CY, Yang KC, Hsieh BC. A comparative study for evaluating the binding affinity of MARAS-selected aptamer and a patented aptamer towards aflatoxin B1 by electrochemical impedimetric aptasensing. *Int J Electrochem Sci*. 2023;18(10):100307. doi:10.1016/j.ijoes.2023.100307
4. Yang CH, Tsai CH. Aptamer against Aflatoxin B1 Obtained by SELEX and Applied in Detection. *Biosensors (Basel)*. 2022;12(10):848. doi:10.3390/bios12100848
5. ZHANG Min ZXLCGHLJTYMWLYTJ. Screening of Aptamers for Aflatoxin B1 and Establishment of a Method for Aflatoxin B1 Detection. *Food Science*. 2020;41(24):295-303.
6. Malhotra S, Pandey AK, Rajput YS, Sharma R. Selection of aptamers for aflatoxin M1 and their characterization. *Journal of Molecular Recognition*. 2014;27(8):493-500. doi:10.1002/jmr.2370
7. Ma X, Wang W, Chen X, et al. Selection, identification, and application of Aflatoxin B1 aptamer. *European Food Research and Technology*. 2014;238(6):919-925. doi:10.1007/s00217-014-2176-1
8. Le LCCAJAPGA. Dna ligands for aflatoxin and zearalenone. Published online 2012.
9. Setlem K, Mondal B, Ramlal S, Kingston J. Immuno Affinity SELEX for Simple, Rapid, and Cost-Effective Aptamer Enrichment and Identification against Aflatoxin B1. *Front Microbiol*. 2016;7. doi:10.3389/fmicb.2016.01909
10. Wei X, Ma P, Imran Mahmood K, Zhang Y, Wang Z. Screening of a High-Affinity Aptamer for Aflatoxin M1 and Development of Its Colorimetric Aptasensor. *J Agric Food Chem*. 2023;71(19):7546-7556. doi:10.1021/acs.jafc.3c01586
11. Liu R, Zhang F, Sang Y, Liu M, Shi M, Wang X. Selection and Characterization of DNA Aptamers for Constructing Aptamer-AuNPs Colorimetric Method for Detection of AFM1. *Foods*. 2022;11(12):1802. doi:10.3390/foods11121802